Numerical analyses of cracks in piezoelectric composite structures under electromechanical loading

Matthias Scherzer Meinhard Kuna
TU Bergakademie Freiberg, Institut für Mechanik und Maschinenelemente
Lampadiusstraße 4, D-09596 Freiberg, Germany

Abstract

The present work is directed to the analysis of interface corner and crack configurations which occur in smart materials. It delivers a new technique for solving the corresponding piezoelectric boundary value problems by asymptotic eigenfunction expansions in connection with the conventional finite element method. This approach represents the extension to coupled electromechanical material behaviour of a method which was introduced in former times for geometrical and physical linear and non-linear solid mechanics [6].

Piezoelectric, ferroelectric and dielectric ceramics or polymers are widely applied in Micro Electro Mechanical Systems (MEMS) to supply the essential sensing and/or actuating functionality [3, 5]. As a consequence of their integration into MEMS, these smart materials may be exposed to extraordinary high mechanical and/or electrical static, dynamic or cyclic loading. Therefore, problems of fracture and fatigue play an important role for the optimum design and reliable service performance of MEMS. Fracture mechanics analyses and safety concepts have to be applied to crack-like defects in piezoelectric bulk materials or in interface structures.

1 Linear Piezoelectricity and asymptotic analysis

First theoretical studies [2, 4] about the asymptotic behaviour at interface crack tips in piezoelectrics show that difficult singular oscillatory solutions can occur. To take into consideration this complicated feature in real boundary value problems and to develop associated stable numerical methods for its handling, it is necessary to dispose of the complete eigenfunction expansions at interface and corner crack tips. Generating these expansions we will at first discuss the used basic relations of piezoelectricity. It is clear that the starting point can include only the simplest approach for both material domains of the interface configuration. The main assumptions are mentioned in the following points:

1. Neglegting of magnetic and time rate effects
2. Introducing the thermomechanical-electric coupling by the electric energy term in the first law of theromodynamics
3. Linearization on the electric hysteresis loop
4. Transversal isotropic piezoelectric behaviour

The governing relations describing this linear piezoelectricity represent the equations of stress equilibrium, the compatibility equations and Gauss' law of electrostatics

$$\sigma_{ij,i} = 0,\ S_{ij} = \tfrac{1}{2}(u_{i,j} + u_{j,i}),\ D_{i,i} = 0, \quad \text{(i,j=1,2,3)} \tag{1}$$

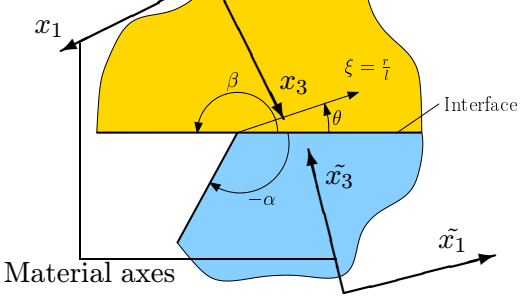

Figure 1: Interface corner configuration

as well as the material equations of the electromechanical interaction:

$$\begin{aligned}
\sigma_{11} &= c_{11}S_{11} + c_{12}S_{22} + c_{13}S_{33} - e_{31}E_3,\ \sigma_{21} = (c_{11} - c_{12})S_{21} \\
\sigma_{22} &= c_{12}S_{11} + c_{11}S_{22} + c_{13}S_{33} - e_{31}E_3,\ \sigma_{13} = 2c_{44}S_{13} - e_{15}E_1 \\
\sigma_{33} &= c_{13}S_{11} + c_{13}S_{22} + c_{33}S_{33} - e_{33}E_3,\ \sigma_{32} = 2c_{44}S_{32} - e_{15}E_2 \\
D_1 &= 2e_{15}S_{13} + \kappa_{11}E_1,\ D_2 = 2e_{15}S_{32} + \kappa_{11}E_2 \\
D_3 &= e_{31}S_{11} + e_{31}S_{22} + e_{33}S_{33} + \kappa_{33}E_3.
\end{aligned} \tag{2}$$

In (1) and (2) σ_{ij}, S_{ij}, u_i, E_i and D_i denote the stress and deformation tensor, the components of the displacement vector, the negativ gradient of the electrical potential ϕ and the dielectric displacements, respectively. The material parameters c_{ij} (mechanical), e_{ij} (piezoelectric) and κ_{ij} (dielectric) characterize transversly isotropic piezoelectrics with pooling-axis along the third direction of the chosen material co-ordinate system in (2). These material equations are written with regard to the material axes of each material corner domain as shown in Fig. 1 (x_1–x_3, $\tilde{x_1}$–$\tilde{x_3}$). The axes x_2 and $\tilde{x_2}$ are directed perpendicular to the plane of Fig. 1.

Further simplifications lead to two-dimensional statements with the assumptions of plane strain:

$$S_{22} = S_{32} = S_{12} = E_2 = 0\ (x_2 - \text{direction normal to the plane strains}) \tag{3}$$

and reduce the system (1) and (2) to

$$\begin{Bmatrix} S_{11} \\ S_{33} \\ S_{13} \end{Bmatrix} = \begin{pmatrix} a_{11} & a_{13} & 0 \\ a_{13} & a_{33} & 0 \\ 0 & 0 & \frac{d_{33}}{2} \end{pmatrix} \begin{Bmatrix} \sigma_{11} \\ \sigma_{33} \\ \sigma_{13} \end{Bmatrix} + \begin{pmatrix} 0 & b_{13} \\ 0 & b_{33} \\ \frac{b_{31}}{2} & 0 \end{pmatrix} \begin{Bmatrix} D_1 \\ D_3 \end{Bmatrix} \tag{4}$$

$$\begin{Bmatrix} E_1 \\ E_3 \end{Bmatrix} = -\begin{pmatrix} 0 & 0 & b_{31} \\ b_{13} & b_{33} & 0 \end{pmatrix} \begin{Bmatrix} \sigma_{11} \\ \sigma_{33} \\ \sigma_{13} \end{Bmatrix} + \begin{pmatrix} \delta_{11} & 0 \\ 0 & \delta_{33} \end{pmatrix} \begin{Bmatrix} D_1 \\ D_3 \end{Bmatrix} \tag{5}$$

$$\frac{\partial \sigma_{11}}{\partial x_1} + \frac{\partial \sigma_{13}}{\partial x_3} = 0,\ \frac{\partial \sigma_{13}}{\partial x_1} + \frac{\partial \sigma_{33}}{\partial x_3} = 0,\ \frac{\partial D_1}{\partial x_1} + \frac{\partial D_3}{\partial x_3} = 0 \tag{6}$$

$$\frac{\partial^2 S_{11}}{\partial x_3^2} + \frac{\partial^2 S_{33}}{\partial x_1^2} = 2\frac{\partial^2 S_{13}}{\partial x_1 \partial x_3},\ \frac{\partial E_1}{\partial x_3} - \frac{\partial E_3}{\partial x_1} = 0, \tag{7}$$

whereby the coefficients a_{11}, ..., b_{13}, ..., δ_{11} and δ_{33} ($b_{13} \neq b_{31}$) can be determined from the material parameters introduced above.

In the material co-ordinate systems the solution can be searched in form of the potentials $U(x_1, x_3)$ and $\chi(x_1, x_3)$ [7]:

$$\begin{aligned}
\sigma_{11} &= U(x_1, x_3)_{,33},\ \sigma_{33} = U(x_1, x_3)_{,11},\ \sigma_{13} = -U(x_1, x_3)_{,13} \\
D_1 &= \chi(x_1, x_3)_{,3},\ D_3 = -\chi(x_1, x_3)_{,1}.
\end{aligned} \tag{8}$$

of this equation and therewith also the solution of the whole problem - because $\chi(x_1, x_3)$ follow from $U(x_1, x_3)$ by integration - has the form

$$U(x_1, x_3) = \sum_k \sum_{i=1}^{6} d_i(\lambda_k)(x_1 + \tau_i x_3)^{\lambda_k}. \tag{9}$$

The complex variables $d_i(\lambda_k)$ are free coefficients to be determined from the overall solution and τ_i stand for the roots of the characteristic polynom (sixth order with real coefficients) of the partial differential equation. The numbers λ_j which are in general complex ones represent the roots of the the solvability condition of the interface corner configuration together with the associated boundary and transmission conditions.
For each complex root τ_i there exists the corresponding conjugate complex root. Because $U(x_1, x_3)$ is a real function, for the pair of τ_i and $\overline{\tau_i}$ in (9) occur terms of the form

$$\begin{aligned} & e_i p^{\lambda_k} \cos\left[\lambda_k(\kappa + \tfrac{\pi}{2})\right] + f_i p^{\lambda_k} \sin\left[\lambda_k(\kappa + \tfrac{\pi}{2})\right] \\ & \text{with } p = \sqrt{(x_1)^2 + 2\tau_i^r x_1 x_3 + (x_3)^2[(\tau_i^i)^2 + (\tau_i^r)^2]},\ \kappa = \arctan \tfrac{x_1 + \tau_i^r x_3}{\tau_i^i x_3} \\ & \tau_i = \tau_i^r + \sqrt{-1}\tau_i^i,\ d_i(\lambda_k) = e_i(\lambda_k) + \sqrt{-1} f_i(\lambda_k). \end{aligned} \tag{10}$$

The solution representation above is valid for each material domain of the interface configuration which has its own material parameters, axes, τ_i and $d_i(\lambda_k)$. The construction of the associated eigenfunction expansion results in the following steps:

1. Transformation of the solutions (9) into the same polar co-ordinate system (ξ, θ) for both material regions ($0 \le \theta \le \beta$ and $0 \ge \theta \ge -\alpha$) of the interface corner configuration

2. Establishing the transcendental solvability condition according to the boundary and transmission conditions

$$\Rightarrow\ Det(\lambda, ...) = 0 \tag{11}$$

   The boundary and transmission conditions have the usual form:
   - Vanishing normal and tangent stresses ($\sigma_{\theta\theta}, \sigma_{\xi\theta}$) and vanishing normal dielectric displacements (D_θ) at $\theta = \beta,\ \theta = -\alpha$
   - Continuity of normal and tangent stresses, both displacement components (u_ξ, u_θ), electric potential (ϕ, $E_1 = -\frac{\partial \phi}{\partial x_1}$, $E_3 = -\frac{\partial \phi}{\partial x_3}$) and normal dielectric displacements at $\theta = 0$
   Modifications of these boundary conditions are not essential for the application of the following solution technique. The only requirements are that they must result from physical reasons and have to give correct formulated problems.

3. Numerical determination of λ: $\Rightarrow \lambda_k, k = 1, ..., \infty$ in (11)

4. For complex roots $\lambda_k = \nu_k + \mathrm{i}\mu_k$ the conjugate complex root $\overline{\lambda_k} = \nu_k - \mathrm{i}\mu_k$ exists:
   $\Rightarrow$ terms of the quality $\xi^{\nu_k} \cos(\mu_k ln(\xi)),\ \xi^{\nu_k} \sin(\mu_k ln(\xi))$ occur

5. Determination of the associated eigenvectors and eigenfunctions (and removing of the energetic "useless" functions) to get the expansions

$$U(\xi, \theta) = \sum_{k=1}^{\infty} C_k \xi^{\lambda_k} f_k^{(U)}(\theta, \lambda_k),\ \sigma_{\xi\xi}(\xi, \theta) = \sum_{k=1}^{\infty} C_k \xi^{\lambda_k} f_{k\xi\xi}^{(\sigma)}(\theta, \lambda_k), ... \tag{12}$$

   with the unknown coefficients C_k

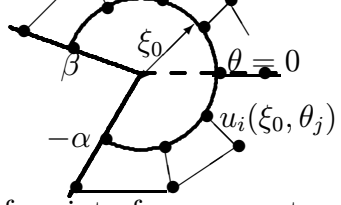

Figure 2: Neighbourhood of an interface corner together with the finite element nodes

2 Replacement of the near tip solutions by asymptotic stiffness matrices

For solving whole boundary value problems of structural elements having interface corner configurations the sole knowledge of the eigenfunctions introduced above is insufficient. The asymptotic eigenfunction expansion in the neighbourhood of the interface corner tip must be connected to the solution of the solid surrounding the interface corner. Doing this at a distance of $\xi = \xi_0$ from the corner finite element nodes of a regular net are established together with the degrees of freedom $u_i(\xi_0, \theta_j)$ for the displacements and the electric potential ϕ (see Fig. 2).

The main idea of the presented approach at interface corners (which was developed in [6] for pure mechanical behaviour) consists in a replacement of the corner neighbourhood ($\xi < \xi_0$) effect to the surrounding body ($\xi > \xi_0$) by introducing of a special stiffness matrix at $\xi = \xi_0$ which can be assembled in a conventional way together with the other element stiffness matrices to the global stiffness matrix. For $\xi < \xi_0$ the following relations are valid:

$$\begin{aligned} \boldsymbol{\sigma} &= \sum_k C_k \mathbf{f}_k^{(\sigma)}(\xi, \theta), \quad \boldsymbol{\sigma} = \{\sigma_{\xi\xi},\ \sigma_{\xi\theta},\ D_\xi\} \\ \mathbf{u} &= \sum_k C_k \mathbf{f}_k^{(u)}(\xi, \theta), \quad \mathbf{u} = \{u_\xi,\ u_\theta,\ \phi\}. \end{aligned} \tag{13}$$

In (13) the marks $\mathbf{f}_k^{(u)}(\xi, \theta) = \{f_{k\xi}^{(u)}(\xi, \theta), f_{k\theta}^{(u)}(\xi, \theta), f_k^{(\phi)}(\xi, \theta)\}$ and $\mathbf{f}_k^{(\sigma)}(\xi, \theta) = \{f_{k\xi\xi}^{(\sigma)}(\xi, \theta), f_{k\xi\theta}^{(\sigma)}(\xi, \theta), f_{k\xi}^{(D)}(\xi, \theta)\}$ denote the corresponding vectors of the displacement and stress eigenfunctions whose concrete forms follow from the eigenfunction expansion above. The constants C_k can be related to the degrees of freedom $u_i(\xi_0, \theta_j)$ ($u_1(\xi_0, \theta_j) = u_\xi(\xi_0, \theta_j)$, $u_2(\xi_0, \theta_j) = u_\theta(\xi_0, \theta_j)$, $u_3(\xi_0, \theta_j) = \phi(\xi_0, \theta_j)$) by

$$\begin{aligned} u_\xi(\xi_0, \theta_j) &= \sum_k C_k f_{k\xi}^{(u)}(\xi_0, \theta_j), \\ u_\theta(\xi_0, \theta_j) &= \sum_k C_k f_{k\theta}^{(u)}(\xi_0, \theta_j), \\ \phi(\xi_0, \theta_j) &= \sum_k C_k f_k^{(\phi)}(\xi_0, \theta_j),\ (j = 1, 2, 3, ...) \end{aligned} \tag{14}$$

and solving (14) one gets

$$\begin{aligned} C_k &= \sum_j b_{kj}(\xi_0, \theta_1, ...) v_j(\xi_0),\ \theta_1 = -\alpha, ...\theta_N = \beta, \\ & v_1(\xi_0) = u_\xi(\xi_0, \theta_1), v_2(\xi_0) = u_\theta(\xi_0, \theta_1), v_3(\xi_0) = \phi(\xi_0, \theta_1), \\ & v_4(\xi_0) = u_\xi(\xi_0, \theta_2), v_5(\xi_0) = u_\theta(\xi_0, \theta_2), v_6(\xi_0) = \phi(\xi_0, \theta_2), \\ & v_7(\xi_0) = u_\xi(\xi_0, \theta_3), ... \end{aligned} \tag{15}$$

To obtain the stiffness matrix it is necessary to calculate the virtual work δA of the stresses $\boldsymbol{\sigma}$ at the virtual displacements $\delta\mathbf{u}$ on the circle $\xi = \xi_0$:

$$\delta A = \xi_0 \int_{-\alpha}^{\beta} \boldsymbol{\sigma} \bullet \delta\mathbf{u}\, d\theta = \sum_{j,l} q_{jl} v_j(\xi_0) \delta v_l(\xi_0),$$

$$q_{jl} = \xi_0 \sum_{i,k} b_{ij} b_{kl} \int_{-\alpha} \mathbf{f}_i^{(\sigma)}(\xi_0, \theta) \bullet \mathbf{f}_k^{(u)}(\xi_0, \theta)\, d\theta \tag{16}$$

The symbol "$\bullet$" marks scalar products of the corresponding vectors. The jl (j-th column, l-th row) element of the wanted stiffness matrix is determined in (16) as the factor of $v_j(\xi_0)\delta v_l(\xi_0)$ i.e. q_{jl}. Computations of these stiffnesses by (16) requires to use n eigenfunctions if n degrees of freedom exist at $\xi = \xi_0$. Avoiding this non-effective procedure it is possible and necessary to orthogonalize the eigenfunctions.

3 Orthogonalization of eigenfunctions

The orthogonalization procedure is analogous to the technique given in [6]. Therefore, here the final formulas will be presented only. After orthogonalization the virtual work δA, the stresses und displacements at $\xi = \xi_0$ result in:

$$\mathbf{u}(\xi, \theta)_{|\xi=\xi_0} = \sqrt{\xi_0} \sum_k \overline{C_k} \overline{\mathbf{f}_k^{(u)}}(\theta),\ \boldsymbol{\sigma}(\xi, \theta)_{|\xi=\xi_0} = \tfrac{1}{\sqrt{\xi_0}} \sum_k \overline{C_k} \overline{\mathbf{f}_k^{(\sigma)}}(\theta), \tag{17}$$

$$\delta A = \xi_0 \sum_k \pm \overline{C_k} \delta \overline{C_k},\ \overline{C_k} = \pm \int_{-\alpha}^{\beta} \overline{\mathbf{f}_k^{(\sigma)}}(\theta) \bullet \tfrac{\mathbf{u}(\xi_0, \theta)}{\sqrt{\xi_0}} d\theta. \tag{18}$$

The vector functions $\overline{\mathbf{f}_k^{(\sigma)}}(\theta)$ and $\overline{\mathbf{f}_j^{(u)}}(\theta)$ fulfil the condition

$$\int_{-\alpha}^{\beta} \overline{\mathbf{f}_k^{(\sigma)}}(\theta) \bullet \overline{\mathbf{f}_j^{(u)}}(\theta)\, d\theta = \pm \delta_{kj}. \tag{19}$$

Note that the coefficients $\overline{C_k}$ depend on ξ_0 ($\overline{C_k} = \overline{C_k}(\xi_0)$) while C_k are constants. The sign in (18) and (19) depends on the integrals over the basic eigenfunctions in (12). The negative signs which can occur in (18) and (19) imply the non-positive definiteness of piezoelectric problems. The relations (18) allow an excellent determination of the wanted stiffness matrix in δA after a possible choice of the $\theta-$ finite element approximation for the displacements $\mathbf{u}(\xi_0, \theta)$:

$$\mathbf{u}(\xi_0, \theta) = \sum_j \mathbf{N}_j(\theta) v_j(\xi_0),$$

with $\mathbf{N}_j(\theta)$ as the one-dimensional vector shape functions at the circle $\xi = \xi_0$. Then δA gets the representation:

$$\delta A = \sum_{j,l,k} \pm \hat{q}_{kj} \hat{q}_{kl} v_j(\xi_0) \delta(v_l(\xi_0)),\ \hat{q}_{kj} = \int_{-\alpha}^{\beta} \left(\overline{\mathbf{f}_k^{(\sigma)}}(\theta)\ \bullet \mathbf{N}_j(\theta) \right) d\theta. \tag{20}$$

Thus the wanted stiffness elements q_{jl} can be calculated by:

$$q_{jl} = \sum_k \pm \hat{q}_{kj} \hat{q}_{kl}. \tag{21}$$

The interesting feature of q_{jl} is their independence of ξ_0 which repeat the findings of the pure mechanical case [6].

The complete stiffness matrix of the whole solid can be assembled by the help of usual finite elements and q_{jl} taking into consideration the special asymptotic behaviour at interface corner tips. After determination of the FEM-solution $\mathbf{u}$ is known for whole solid and at $\xi = \xi_0$. The coefficients $\overline{C_k}$ follow from (18). The calculation of the constants C_k is possible by means of (13) and (18) with:

$$\mathbf{u}(\xi, \theta) = \sum_k C_k \mathbf{f}_k^{(u)}(\xi, \theta). \tag{22}$$

$\sqrt{-1})$, $\lambda_4 = \nu_3 - \mu_3 i, ..., \ \nu_1 < \nu_2 < \nu_3 ...$ the following system of equations is valid:

$$\begin{aligned}
\overline{C_1} &= \xi_0^{\nu_1+\frac{1}{2}} K_{11} C_1 + \xi_0^{\nu_2+\frac{1}{2}} K_{12} C_2 + \xi_0^{\nu_3+\frac{1}{2}} (K_{13} C_3 + K_{14} C_4) + ... \\
\overline{C_2} &= \xi_0^{\nu_2+\frac{1}{2}} K_{22} C_2 + \xi_0^{\nu_3+\frac{1}{2}} (K_{23} C_3 + K_{24} C_4) + ... \\
\overline{C_3} &= \xi_0^{\nu_3+\frac{1}{2}} (K_{33} C_3 + K_{34} C_4) + ... \\
\overline{C_4} &= \xi_0^{\nu_3+\frac{1}{2}} K_{44} C_4 + ... \\
: &= : \qquad (23)
\end{aligned}$$

In (23) the quantities $K_{ij} = K_{ij}(g_{kl})$ in general depend on the integrals g_{kl} over the scalar product of the functions $\mathbf{g}_k^{(\sigma)}(\theta)$ and $\mathbf{g}_l^{(u)}(\theta)$ which are the θ-dependent parts of the initial eigenfunctions $\mathbf{f}_k^{(u)}(\xi, \theta)$ and $\mathbf{f}_l^{(\sigma)}(\xi, \theta)$ by:

$$g_{kl} = \int_{-\alpha}^{\beta} \mathbf{g}_k^{(\sigma)}(\theta) \bullet \mathbf{g}_l^{(u)}(\theta) d\theta.$$

The fact that $K_{21} = K_{31} = K_{32} = K_{41} = ... = 0$ is a consequence of the orthogonalized eigenfunction system construction. This way the solution for the whole solid and the corner region is determind.

On the other hand it is interesting to note the ξ_0-dependence of the solution which follows from (17) and (23):

$$\mathbf{u}(\xi_0, \theta) = \xi_0 \sum_k D_k \xi_0^{\nu_k} (1 + d_{kk+1} \xi_0^{(\nu_{k+1} - \nu_k)} + ...) \overline{\mathbf{f}_k^{(u)}}(\theta)$$

$$\boldsymbol{\sigma}(\xi_0, \theta) = \sum_k D_k \xi_0^{\nu_k} (1 + d_{kk+1} \xi_0^{(\nu_{k+1} - \nu_k)} + ...) \overline{\mathbf{f}_k^{(\sigma)}}(\theta)$$

$$D_k = K_{kk} C_k, \ d_{ki} = \frac{K_{ki} C_i}{D_k}$$

In this parameter dependence we have no oscillation effects even if the solvability condition (11) produces complex roots and the "strong" solution includes the trigonometric-logarithmic terms mentioned above. Therefore, the proposed numerical aqpproach has two advantages:

1. the asymptotic stiffness matrix does not depend on ξ_0 (invariance)
2. the oscillating terms are circumvented numerically but still contained fully

This makes it possible to "live" with the oscillatory asymptotic solution of the interface crack tip also. Since the coefficients of the eigenfunctions completely describe the electromechanical fields in the interface corner region they can be handled as fracture parameters and used to formulate failure criteria.

4 First test example

The procedure of asymptotic stiffness matrix calculations was realized by the help of modern computer algebra systems and implemented together with the commercial finite element code ABAQUS [1].

Results of test computations will be explained. An interface crack specimen (Fig. 3) of two different piezoelectric materials (100*200 dimensionless extension, crack in the middle of the specimen with a length of 50, plane strain (3) conditions) is strained homogenously at the upper specimen end and clamped right opposite. The electric potential is given at the right specimen side ($x_1 = 50, \ -100 \leq x_3 \leq 100$) with zero values.

For this specimen the following material parameters are introduced:

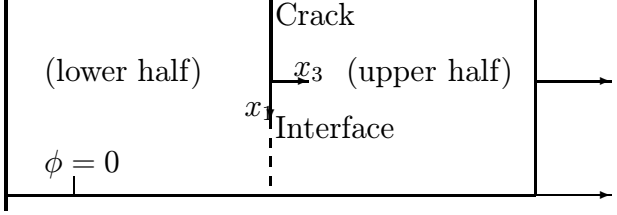

Figure 3: Piezoelectric specimen under tension

Upper half (PZT-4):

$c_{11} = 1.39 * 10^{11} \frac{N}{m^2}$, $c_{33} = 1.13 * 10^{11} \frac{N}{m^2}$, $c_{12} = 7.78 * 10^{10} \frac{N}{m^2}$, $c_{13} = 7.43 * 10^{10} \frac{N}{m^2}$, $c_{44} = 2.56 * 10^{10} \frac{N}{m^2}$
$\kappa_{11} = 6.0 * 10^{-9} \frac{C}{Vm}$, $\kappa_{33} = 5.470 * 10^{-9} \frac{C}{Vm}$, $e_{15} = 13.44 \frac{C}{m^2}$, $e_{31} = -6.98 \frac{C}{m^2}$, $e_{33} = 13.84 \frac{C}{m^2}$

Lower half (hypothetical):

$c_{11} = 2.39 * 10^{11} \frac{N}{m^2}$, $c_{33} = 1.13 * 10^{10} \frac{N}{m^2}$, $c_{12} = 4.78 * 10^{10} \frac{N}{m^2}$, $c_{13} = 5.43 * 10^{10} \frac{N}{m^2}$, $c_{44} = 2.56 * 10^{10} \frac{N}{m^2}$
$\kappa_{11} = 4.0 * 10^{-9} \frac{C}{Vm}$, $\kappa_{33} = 2.470 * 10^{-9} \frac{C}{Vm}$, $e_{15} = 12.0 \frac{C}{m^2}$, $e_{31} = -4.98 \frac{C}{m^2}$, $e_{33} = 14.0 \frac{C}{m^2}$

From these material parameters which have the same pooling directions (x_3) in both material domains and for the homogenous boundary and transmission conditions given above the roots λ_k of the solvability condition (11) result in:

1. $-0.5 \pm \sqrt{-1} * 0.117327$, $0.5 \pm \sqrt{-1} * 0.117327$, $1.5 \pm \sqrt{-1} * 0.117327$, ...
2. -0.5, 0.5, 1.5, 2.5, ...
3. 0.0, 1.0, 2.0, 3.0, ...

Each pair of the conjugate complex roots (1.) produces two linear independent eigenvectors from the free constants $d_i(\lambda_k)$ while the second part of the roots (2.) have single eigenvectors and the third part (3.) generates three linear independent eigenvectors for each concrete value. In Fig. 4 the stress components σ_{33} and σ_{13} together with the electric field E_3 are represented according to a zoom radius $\xi_z = 1.0$. The solutions of usual finite element computations ("without asymptotics") are compared with solutions following from the technique introduced above ("with asymptotics", $\xi_0 = 0.01$). The crack tip lies in the centre and the interface on the horizontal straight line (x_1-axis) on the right side as prolongation of the crack. The results repeat the fact of pure mechanical calculations [6] that in general the usual finite element method cannot give the correct solution at interface crack tips. The pure finite element representation of σ_{33} is analogous to the asymptotic behaviour at a crack tip inside homogenous isotropic material and cannot "feel" interface tip effects. On the other hand the stress component σ_{13} of this same solution ("without asymptotics") fulfil the given boundary conditions on the crack surfaces in a very bad manner only. The differences between the solutions with and without asymptotics can also be seen on the representations of the electric variables i.e. the electric potential gradient, whereby the solution symmetry according to the x_3-axis is not found in the pure finite element solution. Further detailed and sensitive computations should answer the question for which materials and for which interface corner configurations the usual finite element method is usable and for which not.

References

[1] *ABAQUS Version 5.8.* Hibbitt, Karlsson & Sorensen, Inc. USA 1998.

[2] H.G. Beom and S.N. Atluri: *Near-tip fields and intensity factors for interfacial cracks in dissimilar anisotropic piezoelectric media.* International Journal of Fracture 75(2), pp. 163–183, 1996.

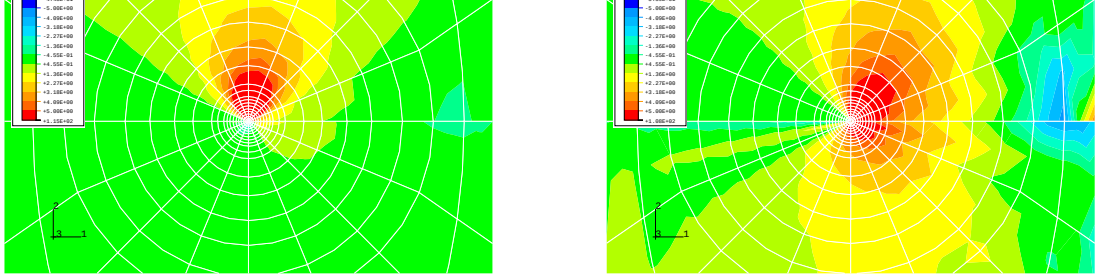

(σ_{33} with asymptotics) (σ_{33} without asymptotics)

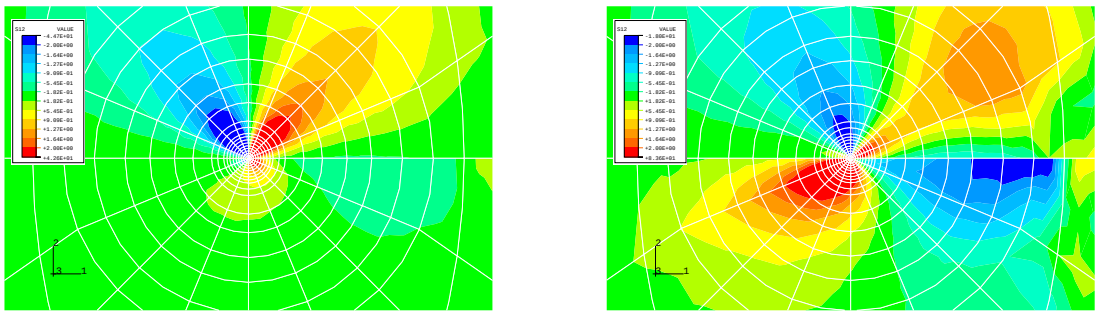

(σ_{13} with asymptotics) (σ_{13} without asymptotics)

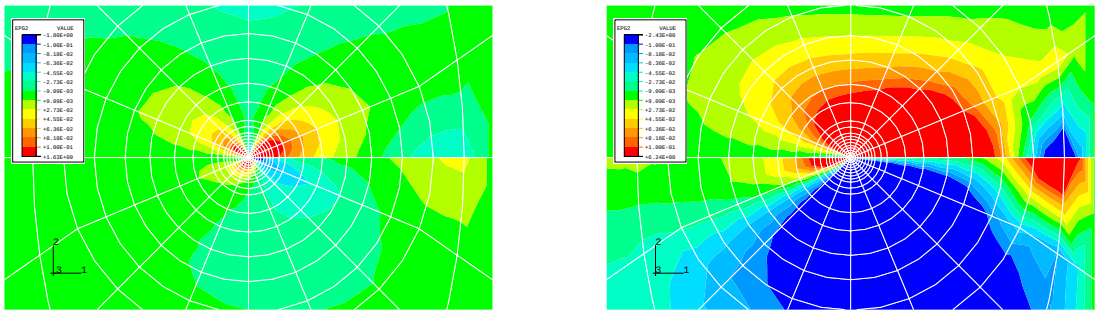

(E_3 with asymptotics) (E_3 without asymptotics)

Figure 4: Piezoelectric solutions at an interface crack tip under tension

[3] A. Heuberger (Editor): *Mikromechanik, Mikrofertigung mit Methoden der Halbleitertechnologie.* Springer-Verlag, Berlin Heidelberg New York, 1991.

[4] C.-M. Kuo and D.M. Barnett: *Stress singularities of interfacial cracks in bonded piezoelectric half-spaces.* In J.J. Wu, T.T.C. Ting and D.M. Barnett, Eds., Modern Theory of Anisotropic Elasticity and Applications, pp. 33–50, Philadelphia 1991. SIAM Proceedings Series.

[5] Qing-Hua Qin, Yiu-Wing Mai and Shou-Wen Yu: *Micromechanics for thermopiezoelectrical materials with microcracks.* In Proceedings of Micro Materials 1997, Berliner Congress Center (BCC), 16-18 April 1997, pp. 352–359, Berlin 1997. Deutscher Verband für Materialforschung und -Prüfung e.V.

[6] M. Scherzer: *Physikalisch und geometrisch nichtlineare Problemstellungen der Festkörper- und Bruchmechanik an Interface-Konfigurationen.* Habilitationsschrift, Technische Universität Bergakademie Freiberg 1999.

[7] H. Sosa: *Plane problems in piezoelectric media with defects.* International Journal of Solids and Structures 28(4), pp. 491–505, 1991.